

# Black Holes Modeled as Fluid Droplets on Membranes

A Senior Project Thesis

By

[REDACTED] Bardessono

Advisor: Dr. Scott Fraser

Department of Physics, California Polytechnic State University, San Luis Obispo

Winter 2016

## Abstract

We examine the known geometry of a black hole on a membrane and propose that its event horizon may be accurately approximated by the profile of a fluid droplet in flat space. The black hole in question varies in size and shape based on a single parameter  $x_r$ , and may be embedded in flat space for a specific range of  $x_r$  values. We compare these embeddings to the shapes of fluid droplets in a uniform gravitational field, and find that the fluid droplet accurately approximates the geometry of the black hole. In the model, two relevant parameters ( $c, d$ ) emerge that determine the shape of the fluid droplet (and thus the accuracy of the match to the black hole's embedding). We find values that best match our black hole's geometry and speculate on directions for future research.

# Contents

<b>1</b>	<b>Introduction</b>	<b>1</b>
<b>2</b>	<b>Black Holes on Membranes</b>	<b>1</b>
2.1	Geometry and Circumference . . . . .	1
2.1.1	The Parameter $x_r$ . . . . .	2
2.1.2	Circumference . . . . .	2
2.2	Embedding in Flat Space . . . . .	4
<b>3</b>	<b>Profile Shapes of Fluid Droplets</b>	<b>6</b>
3.1	Classical Laplace Equation (First-Order Curvature Terms) . . . . .	7
3.2	Generalized Laplace Equation (Second-Order Curvature Terms) . . . . .	8
<b>4</b>	<b>Fitting Embedded Black Holes to Fluid Droplets</b>	<b>9</b>
4.1	Results for Negative Membrane Tension . . . . .	9
4.2	Results for Positive Membrane Tension . . . . .	10
4.3	Parameter Analysis . . . . .	11
<b>5</b>	<b>Conclusions</b>	<b>13</b>
	<b>References</b>	<b>14</b>

# 1 Introduction

Shortly after the discovery (both theoretical, and later observational) of black holes, it has been noted by many experts in the field of general relativity that black holes have many behaviors that are paralleled by fluids. In this thesis, we expand on this observation by examining a specific black hole and recreating its geometry using a known method of plotting the profile shapes of fluid droplets [3, 4]. The black hole we look at has been discussed and examined at length in two previous papers [1, 2]. It sits on a “membrane” (or “brane”) that can have either positive or negative membrane tension. Our black hole sits on this membrane in a way similar to how a fluid droplet would rest on a solid surface.

## 2 Black Holes on Membranes

### 2.1 Geometry and Circumference

From [1, 2], the spatial geometry, both on and outside of our black hole, is given by

$$ds^2 = \frac{\ell^2}{(x-y)^2} \left( \frac{dy^2}{H(y)} + \frac{dx^2}{G(x)} + G(x)d\phi^2 \right), \quad (1)$$

where  $\ell$  is related to the cosmological constant  $\Lambda$  and acts as a scaling factor (this allows us to set  $\ell = 1$  in our numerical plots). The membrane is the surface  $x = 0$ , which intersects the equator of the black hole. The back hole surface is  $y = -1/(2\mu)$ . The constant  $\mu$  characterizes the size of the black hole: a small black has a small value of  $\mu$ , and a large black hole has a large value of  $\mu$ .

The coordinate  $\phi$  is an angle that circles around the black hole’s symmetry axis, with range  $0 \leq \phi \leq \Delta\phi$ . We emphasize that the other coordinates  $(x, y)$  are not the same as in familiar Cartesian coordinate systems. They are analogous to the other two spherical coordinates that go with  $\phi$ . The coordinate  $x$  is analogous to a ‘latitude’ or the cosine of a polar angle. The coordinate  $y$  is analogous to a radial spherical coordinate. The functions in equation 1 are  $G(x) = 1 - x^2 - 2\mu x^3$  and  $H(y) = y^2(1 + 2\mu y)$ , and the parameter  $\mu$  is

$$\mu = \frac{1 - x_r^2}{2x_r^3}, \quad (2)$$

where  $x_r$  is one of the real roots of  $G(x)$ .

### 2.1.1 The Parameter $x_r$

The brane that our black hole sits on contains what is effectively a surface tension. This membrane tension can be either negative or positive. For each type of membrane tension, we use a specific root,  $x_r$ , that satisfies  $G(x_r) = 0$ . In general, the three roots of  $G(x)$  satisfy [1, 2]

$$-\frac{1}{2\mu} < x_0 < x_1 < 0 < x_2. \quad (3)$$

As in [1, 2], for the negative tension brane, we use  $x_r = x_1$ , and for the positive tension brane, we use  $x_r = x_2$ . For each tension,  $x_r$  may take on a range of values. The root  $x_1$  varies from  $-\sqrt{3}$  to  $-1$ , and the root  $x_2$  varies from 0 to 1.

The root  $x_r$  that we use is related to important aspects of the geometry. The black hole's symmetry axis is  $x = x_r$ . The range of the coordinate  $x$  and the value of  $\Delta\phi$  are as follows. For negative membrane tension,  $x_1 \leq x \leq 0$ . For positive membrane tension,  $0 \leq x \leq x_2$ . The value of  $\Delta\phi$  is

$$\Delta\phi = \frac{4\pi x_r}{|x_r^2 - 3|}. \quad (4)$$

Negative and positive tension branes produce qualitatively different-looking black holes. Near one extreme value of  $x_r$ , we find that our black hole becomes very large. Near the other extreme value of  $x_r$  we find that our black hole becomes arbitrarily small.

In sum, we are examining one geometry, equation 1, that produces two related but uniquely-behaving black holes (the black hole with parameter  $x_1$  and the black hole with parameter  $x_2$ ), and each of these black holes may take on a range of sizes.

### 2.1.2 Circumference

We now examine the circumference of our black hole, to get an idea of how it behaves in the positive and negative tension cases and also as the value of  $x_r$  is varied. From [1], the circumference  $C(x)$  is

$$C(x) = \Delta\phi \sqrt{g_{\phi\phi}^H(x)}, \quad (5)$$

where  $\Delta\phi$  is defined in terms of  $x_r$  (see above), and from equation 1, the quantity  $g_{\phi\phi}^H$  is the coefficient of  $d\phi^2$  evaluated at  $y = -1/(2\mu)$ ,

$$g_{\phi\phi}^H(x) = \frac{\ell^2 G(x)}{\left(x + \frac{1}{2\mu}\right)^2}. \quad (6)$$

The resulting plots of the circumference are shown below, Figures 1 and 2. Each plot shows the black hole circumference as a function of  $x$  at a specific value of the parameter  $x_r$ . The solid lines represent values near the extrema of  $x_r$ , while the dashed lines indicate intermediate values.

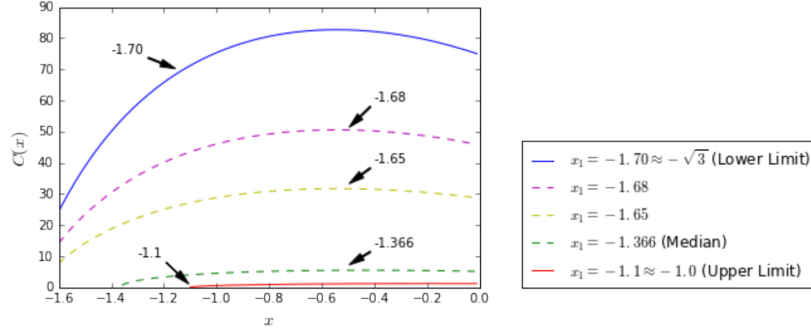


Figure 1: Plot of circumference of a black hole on a negative tension brane for various values of  $x_1$ .

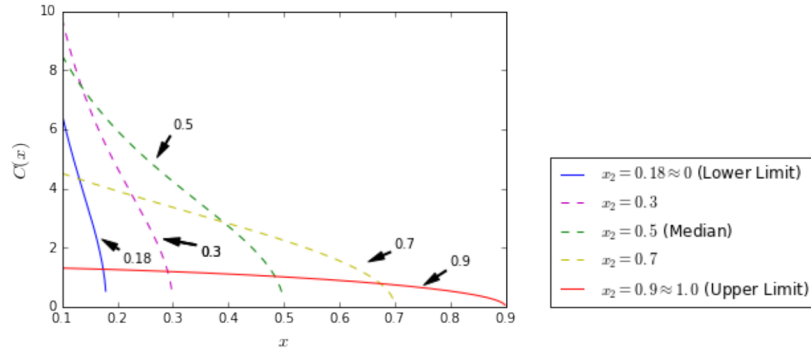


Figure 2: Plot of circumference of a black hole on a positive tension brane for various values of  $x_2$ .

Immediately, we can see that at one extreme of  $x_r$  (the upper limits), our black hole becomes increasingly small. As each  $x_r$  approaches its other extreme value (lower limits), our black hole becomes very large. In both cases, if we were examining the entire black hole surface, we would see two points of smallest (zero) circumference at the poles, and a point of maximum circumference in the exact middle (the equator). However, we see only one point of smallest circumference in either case, so we know that we are only displaying half of the black hole (on one side of the membrane).

For the negative tension case, the circumference begins (at negative  $x$ ) at a minimum value, achieves

a maximum, and then begins decreasing at a slower rate than it was increasing. With enough thought, one can interpret this behavior and guess that the black hole must be similar in shape to that of a fluid droplet ‘beading up’<sup>1</sup> on a surface: both have only one point of minimum circumference, both cut off abruptly at the point of contact with the surface ( $x = 0$ ), and both have regions of decreasing and increasing circumference with different rates of change.

What the positive tension case looks like is harder to interpret. However, now that we are thinking in terms of fluid droplets, we assert that this behaviour should generate a ‘wetting’ effect. Whereas a fluid droplet ‘beads up’ because it is repulsed by the surface it rests on and is attempting to become spherical, a fluid droplet ‘wets’ because it is attracted to the surface and is attempting to flatten itself onto it. We see hints of this behavior in the positive tension case: the black hole’s circumference is maximum at the point of contact with the brane ( $x = 0$ ), then unsteadily decreases to a minimum further from the surface.

## 2.2 Embedding in Flat Space

To get a more direct picture of our black hole and to check if our above intuitions are correct, we now examine embedding diagrams. An embedding is a representation of a black hole in flat (Euclidean) space; in essence we are plotting our black hole as if it were an object resting in flat space. For our purposes, we are only concerned with how the event horizon of our geometry looks. At the horizon, we set  $y = -1/(2\mu)$ , so that  $dy = 0$ , and from equation 1, the geometry of our black hole surface is:

$$ds_{BH}^2 = \frac{\ell^2}{(x + \frac{1}{2\mu})^2} \left( \frac{dx^2}{G(x)} + G(x)d\phi^2 \right). \quad (7)$$

To define an embedding, we must match this geometry to the geometry of a surface in flat space. We use cylindrical coordinates  $(z, r, \theta)$  because they are the most convenient, as in [2]. Thus, the geometry of Euclidean space is:

$$ds_E^2 = dz^2 + dr^2 + r^2 d\theta^2, \quad (8)$$

where  $0 \leq \theta \leq 2\pi$ . We now express  $d\theta$  in terms of  $d\phi$  by writing  $\beta = \frac{d\theta}{d\phi} = \frac{2\pi}{\Delta\phi}$ . We also consider a surface given by  $z(x)$  and  $r(x)$ , so we evaluate the differentials  $dz$  and  $dr$  in terms of  $dx$ . This gives

$$ds_E^2 = \left[ \left( \frac{dz}{dx} \right)^2 + \left( \frac{dr}{dx} \right)^2 \right] dx^2 + \beta^2 r^2 d\phi^2. \quad (9)$$

---

<sup>1</sup>In [2] this ‘beading up’ behavior is described as a ‘low-wetting effect’, however we prefer the phrase ‘beading up’.

To embed, we set equations 7 and 9 equal to each other and match the like differential elements. Doing this we find:

$$[\beta^2 r^2] d\phi^2 = \left[ G(x) \left( \frac{\ell}{J(x)} \right)^2 \right] d\phi^2 \quad (10)$$

and

$$\left[ \left( \frac{dz}{dx} \right)^2 + \left( \frac{dr}{dx} \right)^2 \right] dx^2 = \left[ \left( \frac{\ell}{J(x)} \right)^2 \frac{1}{G(x)} \right] dx^2, \quad (11)$$

where  $J(x) = x + \frac{1}{2\mu}$ . Using equation 10, it is simple to solve for  $r$  in terms of  $x$ :

$$r(x) = \pm \frac{\ell}{\beta} \frac{\sqrt{G(x)}}{J(x)}. \quad (12)$$

We cannot find  $z(x)$  analytically, however we can solve for  $\frac{dz}{dx}$ :

$$\frac{dz}{dx} = \pm \sqrt{\frac{\ell^2}{J(x)^2 G(x)} - \left( \frac{dr}{dx} \right)^2}. \quad (13)$$

From equation 12, we find

$$\frac{dr}{dx} = \pm \frac{\ell}{\beta} \left( \frac{J(x)G'(x) - 2G(x)}{2\sqrt{G(x)}J(x)^2} \right). \quad (14)$$

Plugging this into equation 13 gives us the final result:

$$\frac{dz}{dx} = \pm \ell \sqrt{\frac{1}{J^2 G} - \frac{1}{\beta^2} \left( \frac{(JG' - 2G)^2}{4GJ^4} \right)}. \quad (15)$$

Now it is just a matter of numerical integration to generate the embedding  $z(x)$ . As noted in [2], an embedding is not possible for all values of  $x_r$ , so the ‘largest’ black holes shown are not the largest mathematically possible — they are just the largest we are able to represent in this way. See Figures 3 and 4 for the resulting plots. Contrast the shapes of the large black holes (right side of each figure) to their smaller companions (left side of each figure) to see the ‘beading up’ and ‘wetting’ behaviours mentioned earlier.

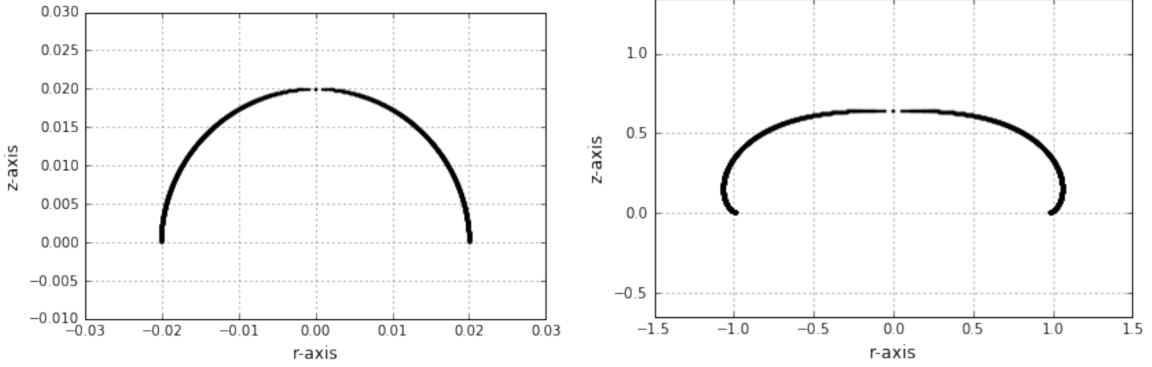


Figure 3: Embedding of a black hole on a negative tension brane for  $x_1 = -1.001$  (left),  $x_1 = -1.41$  (right).

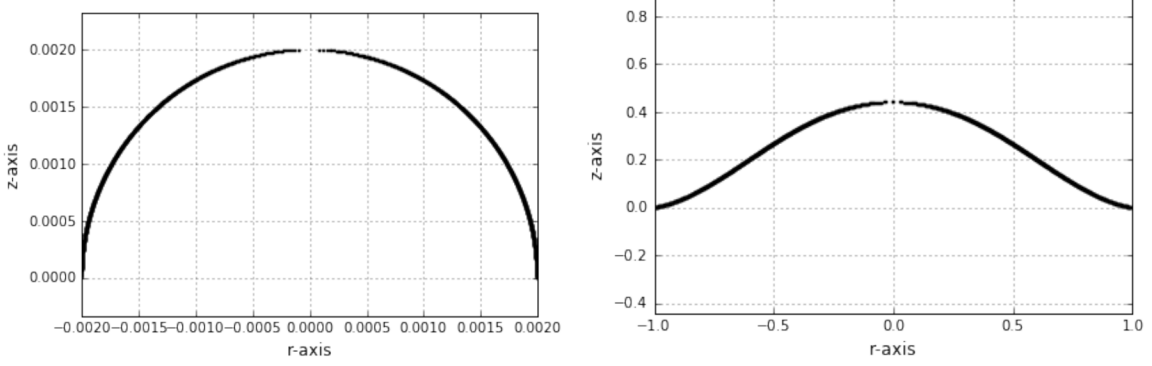


Figure 4: Embedding of a black hole on a positive tension brane for  $x_2 = .99$  (left) and  $x_2 = .663$  (right).

### 3 Profile Shapes of Fluid Droplets

The profile of a fluid droplet in a uniform gravitational field is well known from several references, for example [3]. The profile shape depends on the fluid's surface tension  $\gamma$ , the density pressure difference  $\Delta\rho$  between the droplet and the surrounding fluid or vacuum, and the magnitude  $g$  of the constant gravitational field.

To compare our black hole to a fluid droplet, we examined two models for fluid droplets. The first attempt was the simple model of [3]. I shall refer to this model as the ‘first order model’. The second

model we implemented was proposed in [4], and produced much better results. I shall refer to this model as the ‘second order model’.

### 3.1 Classical Laplace Equation (First-Order Curvature Terms)

Our first attempt to match our black hole to a fluid droplet used the first order model. This model is given by Equation 1 in [3]. In our case, their  $x$  coordinate is our  $r$  coordinate, their  $z$  coordinate is our  $-z$ , and the angle they call  $\theta$  we here shall call  $\alpha$ , to avoid confusion with the angle  $\theta$  in our Euclidean geometry. The first order model then becomes

$$\frac{dr}{ds} = \cos(\alpha), \quad (16a)$$

$$\frac{dz}{ds} = \sin(\alpha), \quad (16b)$$

$$\frac{d\alpha}{ds} = 2b + cz - \frac{\sin(\alpha)}{r}. \quad (16c)$$

Here  $s$  is the arc length along the droplet surface and  $b$  is a curvature parameter defined as  $b = \left. \frac{d^2z}{dr^2} \right|_{r=0}$ , and  $c = \frac{g\Delta\rho}{\gamma}$  is the capillary constant of the system. Numerical methods are needed to solve these equations [3], and are rather straightforward. However, evaluating  $b$  for our black hole geometry is a somewhat lengthy calculation, as this depends on taking  $z(x)$  and  $r(x)$  to be functions of the black hole ‘latitude’ coordinate  $x$ . After doing this,  $\frac{d^2z}{dr^2}$  can be found using the quotient rule:

$$\frac{d^2z}{dr^2} = \frac{d}{dr} \left( \frac{dz}{dr} \right) = \frac{1}{(dr/dx)} \frac{d}{dx} \left( \frac{dz/dx}{dr/dx} \right) = \frac{(dr/dx)(d^2z/dx^2) - (dz/dx)(d^2r/dx^2)}{(dr/dx)^3}. \quad (17)$$

We know  $\frac{dr}{dx}$  from equation 14, and it is simple (although lengthy) calculus exercise to find  $\frac{d^2r}{dx^2}$ . Similarly, we know  $\frac{dz}{dx}$  from equation 15, from which we can find  $\frac{d^2z}{dx^2}$ . I will not write out the steps here (L’Hopital’s rule is needed in the evaluation), but the final result is

$$b = \left. \frac{d^2z}{dr^2} \right|_{r=0} = \frac{x_r \sqrt{2 - x_r^2}}{\ell(1 - x_r^2)}, \quad (18)$$

which was found using Mathematica.

The parameter  $c$  corresponds to physical parameters of a fluid droplet. Numerical values of  $c$  were used to search for good matches between the black hole embedding and the fluid droplet profile.

Using equation 16, our liquid droplet profiles and black holes match well, but only for very small black holes (Figure 5, left). As they become larger, our droplets stop matching (Figure 5, right). If we

increase the parameter  $c$  as we increase the size of our black hole, the matching becomes better further from the apex; however there is always a discrepancy near the point of contact with the brane.

### 3.2 Generalized Laplace Equation (Second-Order Curvature Terms)

Our second order model for fluid droplets was proposed in [4], and has the following form:

$$\gamma(c_1 + c_2) + 2C_1c_1c_2 = \Delta P \quad (19)$$

where  $c_1 = \frac{d\alpha}{ds}$ ,  $c_2 = \frac{\sin(\alpha)}{r}$ ,  $\Delta P = \gamma(2b \pm cz)$  is the pressure difference between the inside and outside of the droplet, and  $C_1$  is a constant. Solving for  $c_1$  and substituting the more familiar form of each term, the equation becomes:

$$\frac{d\alpha}{ds} = \frac{2b + cz - \sin(\alpha)/r}{1 + d\sin(\alpha)/r} \quad (20)$$

where  $d = \frac{2C_1}{\gamma}$  is a new parameter. The full form of our second order model is thus

$$\frac{dr}{ds} = \cos(\alpha) \quad (21a)$$

$$\frac{dz}{ds} = \sin(\alpha) \quad (21b)$$

$$\frac{d\alpha}{ds} = \frac{2b + cz - \sin(\alpha)/r}{1 + d\sin(\alpha)/r} \quad (21c)$$

Note that when  $d = 0$ , we recover the form of our first order model. Various numerical values of  $c$  and  $d$  were found by simple guess and check, and the second order model produced very close matches, for both small and large black holes (the extreme values of  $x_r$ ).

## 4 Fitting Embedded Black Holes to Fluid Droplets

### 4.1 Results for Negative Membrane Tension

Plots comparing fluid droplet profiles and black hole embeddings for a negative tension brane are presented below (Figures 5 and 6). As stated above, the first order model is only accurate for small black holes, while the second order model produced good matches even for some of the largest black holes.

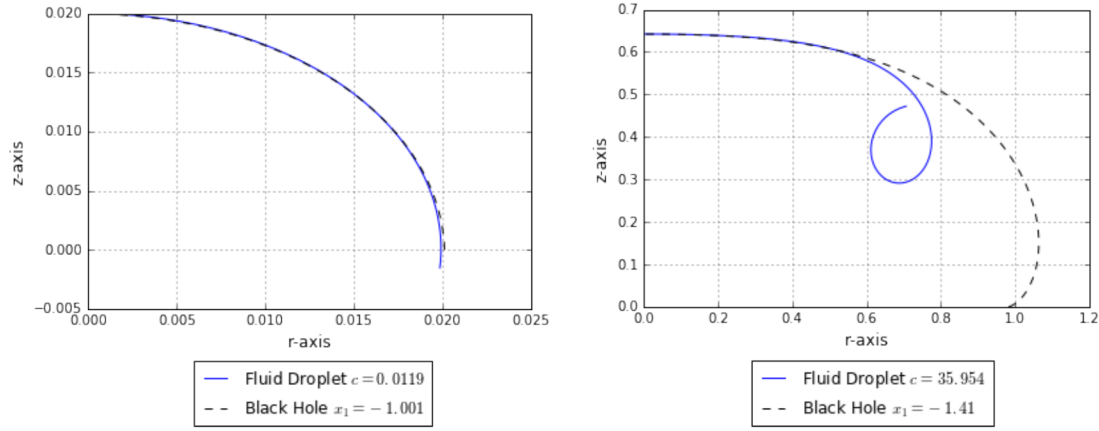


Figure 5: Profile comparison in the first order droplet model of a black hole on a negative tension brane, for a small black hole (left) and a large black hole (right).

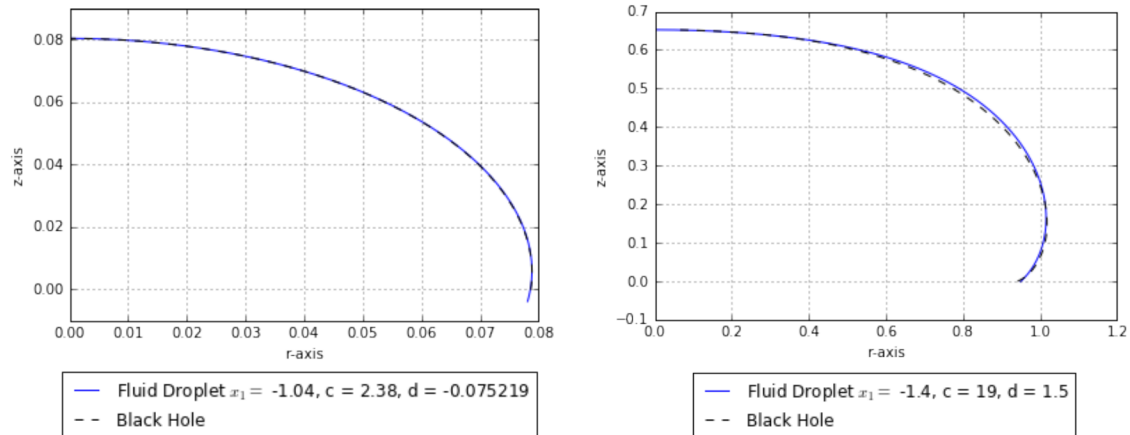


Figure 6: Profile comparison in the second order droplet model of a black hole on a negative tension brane, for a small black hole (left) and a large black hole (right).

## 4.2 Results for Positive Membrane Tension

Plots comparing fluid droplet profiles and black hole embeddings for a positive tension brane are presented below (Figures 7 and 8). Unlike the case of negative tension, the first order model produces good matches for even the largest black holes. The second order model improves upon these slightly.

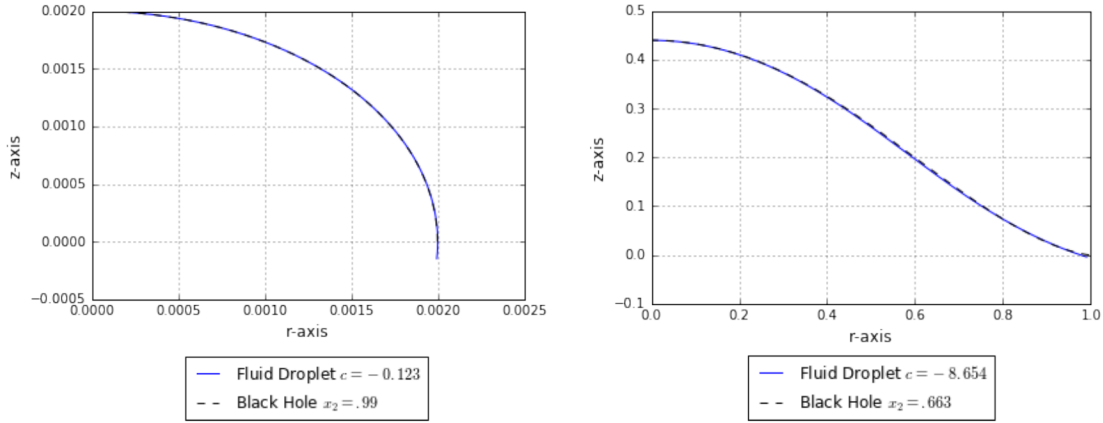


Figure 7: Profile comparison in the first order droplet model of a black hole on a positive tension brane, for a small black hole (left) and a large black hole (right).

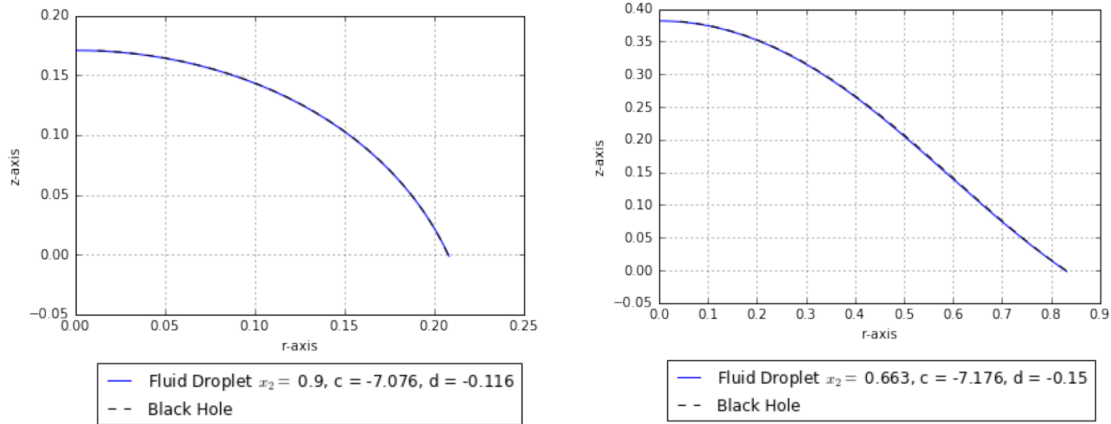


Figure 8: Profile comparison in the second order droplet model of a black hole on a positive tension brane, for a small black hole (left) and a large black hole (right).

### 4.3 Parameter Analysis

This section considers only the results of the second order model. Several numerical values for  $c$  and  $d$  that generated visually good fits are tabulated below. In determining what a ‘good fit’ was, we decided that the best possible droplet profile was one that matched the embedding of the event horizon, starting at the apex, for as far as possible away from the apex.

$x_1$	$d (c = 14)$	$d (c = 2.38)$	$x_2$	$d (c = -7.07664)$
-1.04	-0.05	-0.075219	0.663	-0.23
-1.05	-0.053	-0.09235	0.65	-0.195
-1.06	-0.0515	-0.10953	0.67	-0.146
-1.07	-0.046	-0.127	0.7	-0.12
-1.08	-0.036	-0.1415	0.733	-0.113
-1.09	-0.022	-0.156	0.76	-0.121
-1.10	-0.006	-0.1712	0.833	-0.125
-1.11	0.0183	-0.1845	0.87	-0.125
-1.12	0.046	-0.198	0.9	-0.116
-1.13	0.081	-0.2097	0.933	-0.095
-1.14	0.114	-0.246	0.95	-0.077
-1.15	0.159	-0.235		
-1.16	0.1957	-0.25		
-1.17	0.2585	-0.259		
-1.18	0.3153	-0.271		
-1.19	0.3732	-0.283		
-1.20	0.46	-0.292		
-1.21	0.515	-0.307		
-1.26	0.945	-0.387		
-1.31	1.383	-0.50		

Table 1: Values of parameter  $d$  as a function of  $x_r$  that generated good fits for given values of  $c$ .

In both the positive and negative tension cases, it was found that for a fixed value of  $c$ , some value of  $d$  could be found for each  $x_r$  value that generated a visually good profile fit. For a constant  $c$ , values of  $d$  were taken for several values of  $x_r$ . Least-squares fits of the data were generated, and the resulting plots are shown in Figures 9 and 10. For the case of negative tension,  $d$  appears to be quadratically dependent on  $x_1$ , while for the positive tension case  $d$  appears to be cubically dependent on  $x_2$ .

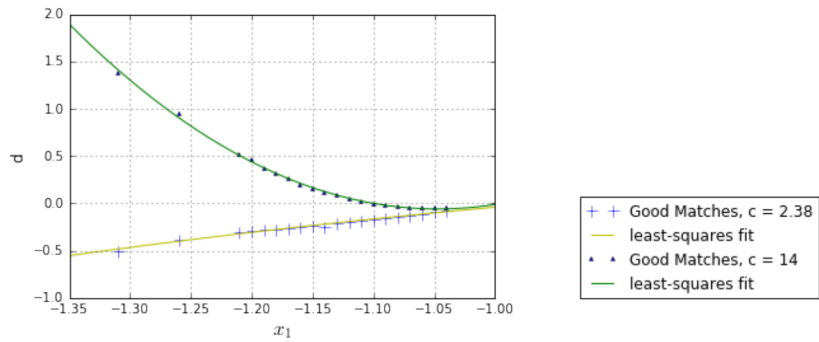


Figure 9: Fits of parameter  $d$  as a function of  $x_1$  at constant  $c$ .

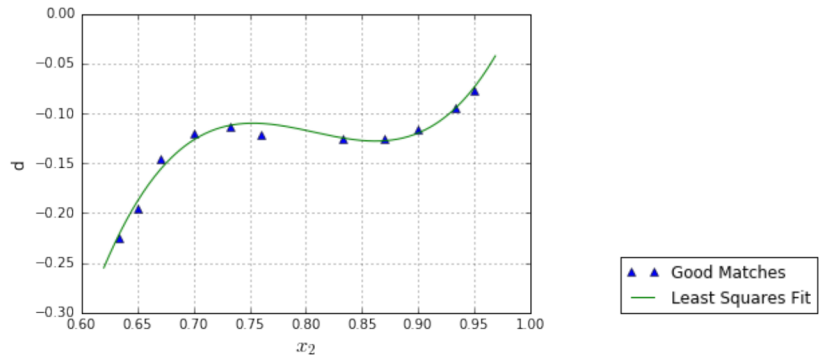


Figure 10: Fit of parameter  $d$  as a function of  $x_2$  for  $c = -7.07664$ .

## 5 Conclusions

Our black hole geometry and fluid droplet profiles match very well for most values of  $x_r$ . However there is always some discrepancy near the point of contact with the brane. We assert that this close matching implies that the fluid droplet and event horizon embedding *should* match, and the model we are using to generate our fluid profiles could be further generalized. The second order model that we used was taken from [4], and is a special case (the parameter  $C_1$  being held constant) of a more general model. The more general model in [4] does not hold  $C_1$  constant. Using this or some other higher order model would, we suspect, generate even better matches. Presumably it would also introduce additional parameters like  $c$  and  $d$ .

For negative tension, the parameter  $d$  appears to be a roughly second-degree polynomial function of  $x_r$  for constant values of  $c$ . For positive tension, parameter  $d$  appears to also have cubic dependence on  $x_r$  for constant  $c$ . It would be interesting to further explore these parameter spaces, or possibly find exact analytical forms of the parameters  $c$  and  $d$ .

## References

- [1] R. Emparan, G. T. Horowitz and R. C. Myers, *Exact description of black holes on branes*, J. High Energy Phys. **01**, 007 (2000).
- [2] R. Emparan and G. Milanesi, *Exact gravitational dual of a plasma ball*, J. High Energy Phys. **08**, 012 (2009).
- [3] O. I. del Rio and A. W. Neumann, *Axisymmetric drop shape analysis: Computational methods for the measurement of interfacial properties from the shape and dimensions of pendant and sessile drops*, J. Colloid Interface Sci. **196**, 136 (1997).
- [4] M. Pasandideh-Fard, P. Chen, J. Mostaghimi and A. W. Neumann, *The generalized Laplace equation of capillarity I: Thermodynamic and hydrostatic considerations of the fundamental equation for interfaces*, Adv. Colloid Interface Sci. **63**, 151 (1996).